AD-771 915

EXCITATION MECHANISMS FOR TRANSMISSION THROUGH FOREST-COVERED AND VEGETATED MEDIA

Randolph H. Ott, et al

Office of Telecommunications

Prepared for:

Army Communications Command

November 1973

DISTRIBUTED BY:

NTIS

National Technical Information Service
U. S. DEPARTMENT OF COMMERCE
5285 Port Royal Road, Springfield Va. 22151

DISPOSITION

Destroy this report when no longer needed. Do not return it to the originator.

DISCLAIMER

The findings in this report are not to be construed as an official Department of the Army position unless so designated by other authorized documents.

The use of trade names in this report does not constitute an official indorsement or approval of the use of such commercial hardware or software. This report may not be cited for purposes of advertisement.

AD-771915

UNCLASSIFIED
Security Classification

DOCUMENT CONTROL DATA - R & D

(Security classification of title, body of abstract and indexing annotation must be entered when the overall report is classified)

1. ORIGINATING ACTIVITY (Corporate author) U. S. Department of Commerce Office of Telecommunications/Institute for Telecommunication Sciences, Boulder, Colorado 80302	2a. REPORT SECURITY CLASSIFICATION UNCLASSIFIED 2b. GROUP

3. REPORT TITLE

Excitation Mechanisms for Transmission Through Forest-Covered and Vegetated Media

4. DESCRIPTIVE NOTES (Type of report and inclusive dates)

5. AUTHOR(S) (First name, middle initial, last name)

Randolph H. Ott
James R. Wait

6. REPORT DATE	7a. TOTAL NO. OF PAGES	7b. NO. OF REFS
November 1973	39	18

8a. CONTRACT OR GRANT NO. b. PROJECT NO. SCC-408-73, dated 18 Jun 73 c. d.	9a. ORIGINATOR'S REPORT NUMBER(S) ACC-ACO-8-73 9b. OTHER REPORT NO(S) (Any other numbers that may be assigned this report)

10. DISTRIBUTION STATEMENT

Approved for public release; distribution unlimited

11. SUPPLEMENTARY NOTES	12. SPONSORING MILITARY ACTIVITY U. S. Army Communications Command Advanced Concepts Office Fort Huachuca, Arizona 85613

13. ABSTRACT

Simple asymptotic expressions are derived for the lateral wave excited by loop and dipole antennas in or above a foliage layer. It is shown that the horizontal magnetic dipole (loop in vertical plane) has signal strengths comparable with the vertical electric dipole provided the moments for the two antennas are normalized so that they have equal radiation resistances in free-space.

DD FORM 1 NOV 65 1473 REPLACES DD FORM 1473, 1 JAN 64, WHICH IS OBSOLETE FOR ARMY USE.

UNCLASSIFIED
Security Classification

14. KEY WORDS	LINK A		LINK B		LINK C	
	ROLE	WT	ROLE	WT	ROLE	WT
Lateral Wave						
Antennas in foliage layer						

ia

Technical Report No. ACC-ACO-8-73

EXCITATION MECHANISMS FOR TRANSMISSION THROUGH FOREST-COVERED AND VEGETATED MEDIA

R. H. Ott and J. R. Wait

U. S. Department of Commerce
Office of Telecommunications
Institute for Telecommunication Sciences
Boulder, Colorado 80302

November 1973

Project Order ACC-408-73 Lateral Wave

Advanced Concepts Office
U. S. Army Communications Command
Fort Huachuca, Arizona 85613

ABSTRACT

Simple asymptotic expressions are derived for the lateral wave excited by loop and dipole antennas in or above a foliage layer. It is shown that the horizontal magnetic dipole (loop in vertical plane) has signal strengths comparable with the vertical electric dipole provided the moments for the two antennas are normalized so that they have equal radiation resistances in free-space.

FOREWORD

An important element of the mission of the Advanced Concepts Office of Headquarters, U. S. Army Communications Command, is to conduct studies whereby scientific knowledge can be utilized in the solution of current or foreseen problems affecting USACC's operational capabilities. This report investigates the problem of radiowave propagation in forested or vegetated media.

This study was conducted by the Institute for Telecommunication Sciences, Office of Telecommunications, U. S. Department of Commerce, Boulder, Colorado, under Project Order SCC-408-73.

Mr. George Lane of USACEEIA was the project monitor supervising this study.

TABLE OF CONTENTS

	ABSTRACT.	ii
	FOREWORD.	iii
	TABLE OF CONTENTS	v
	LIST OF ILLUSTRATIONS	vi
I.	INTRODUCTION.	1
II.	ANALYSIS.	3
III.	NUMERICAL EXAMPLES.	15
IV.	CONCLUSIONS	27
V.	ACKNOWLEDGMENT.	27
	REFERENCES	28
	DISTRIBUTION LIST.	31

LIST OF ILLUSTRATIONS

Figure		Page
1.	Vertical electrical dipole (VED) over N-layered space. The n'th layer of thickness h_n has conductivity σ_{hn} in horizontal direction and σ_{vn} in vertical direction.	4
2.	How the reciprocity theorem is used to calculate the vertical electric field of a horizontal electric dipole (HED).	6
3.	How the reciprocity theorem is used to calculate the vertical electric field of a horizontal magnetic dipole (HMD).	6
4a.	Geometry and parameter values for fig. 4b. Parameters correspond to Jansky and Bailey data.	16
4b.	Normalized magnitude of vertical component of the electric field versus frequency for single-layer model. Three excitation mechanisms are considered; i.e., VED, HED, and HMD.	18
5a.	Geometry and parameter values for figs. 5b, 5c, 5d, and 6. Parameters correspond to Jansky and Bailey data.	19
5b.	Normalized magnitude of vertical component of electric field versus frequency for two-layer model. Three excitation mechanisms are considered; i.e., VED, HED, and HMD. Inference of multiple reflections in upper layer causes the oscillations in calculated data. This fine structure is shown in more detail in the insert for the VED.	21
5c.	Normalized magnitude of vertical component of electric field versus frequency for two locations of the transmitting antenna in fig. 5a.	22
5d.	Normalized magnitude of vertical component of electric field versus frequency for two locations of the receiving antenna in fig. 5a.	23
6.	Basic transmission loss versus frequency for a VED and observer at z=h=0, together with the Jansky and Bailey measured data (1965).	25

EXCITATION MECHANISMS FOR TRANSMISSION
THROUGH FOREST-COVERED AND VEGETATED MEDIA

R. H. Ott and J. R. Wait
U. S. Department of Commerce
Office of Telecommunications
Institute for Telecommunication Sciences
Boulder, Colorado 80302

I. INTRODUCTION

It is now well appreciated that the predominant component of the far-zone field in jungle propagation near the surface is a lateral-type wave. One of the earliest measurements of attenuation by jungles was the work of Herbstreit and Crichlow (1964). Lippmann (1965) modeled Herbstreit's experiments in terms of a plane, uniform slab. Jansky and Bailey Engineering Division (Jones and Sturgill, 1965) conducted a number of experiments in Thailand in 1965. Two of the earliest theoretical interpretations of the attenuation of signals propagating through a jungle are the work of Staiman and Tamir (1966) and Sachs (1966). Since then a number of authors have considered the problem of calculating the lateral wave excited by antennas in a jungle (Wait, 1967a, 1967b, 1968; Sachs and Wyatt, 1968; Dence and Tamir, 1969; Sachs, 1969). A very early theoretical treatment of lateral waves and their relation to other surface waves was the work of Tamir and Felsen (1964). Recently, models of the jungle vegetation have been built and model experiments have been conducted to complement actual field measurements (Ikrath and LeMarne, 1971).

In this report, we derive analytical expressions for the electromagnetic fields of dipole and loop antennas located within a foliage layer over a smooth earth. These expressions are evaluated asymptotically to yield simple formulas for predicting signal strength as a function of the various parameters of the problem. These asymptotic formulas indirectly separate the Hertz vector into its space-wave and lateral-wave components. The location of dipoles and loops in and above a foliage layer is considered to determine the optimum location of the antennas. A comparison of the model with the Jansky and Bailey data is given. At 20 MHz, the measured and predicted basic transmission loss differ by 3 dB. For frequencies greater than 20 MHz, the measured data and theory differ by as much as 18 dB. However, this 18-dB difference remains constant from about 50 MHz to 300 MHz, indicating the theoretical frequency dependence adequately predicts the observer frequency dependence.

The model of the foliage layer can be as simple as a single homogeneous isotropic slab or as complicated as an arbitrary number of homogeneous, uniaxial anisotropic layers. In this analysis we ignore the incoherent or scattered-wave component.

II. ANALYSIS

The general configuration is depicted in fig. 1, where we have an N-layered earth model. Here the top two layers can be used to characterize forested terrain. In general, the complex conductivity is a diagonal tensor given by

$$\begin{pmatrix} \sigma_{hn} & 0 & 0 \\ 0 & \sigma_{hn} & 0 \\ 0 & 0 & \sigma_{vn} \end{pmatrix}$$

for the n'th layer (n = 1,2,....N). Here the complex conductivity $\sigma = g + i\omega\varepsilon$ where g and ε are the real conductivity and the real permittivity, respectively. The implied time factor is $\exp(+i\omega t)$ following Lord Rayleigh. As indicated in fig. 1, the source is a vertical electric dipole, denoted VED, at z = h the vacuum region for z > 0.

For the VED the fields can be derived from an electric Hertz vector that has only a z component Π_z. A subscript o is added when referring to region z > 0, and a subscript n is used for region n where n = 1,2,3,...N. From an earlier analysis (Wait, 1967a), it follows that (for z > 0)

$$\Pi_{oz} = \frac{Ids}{4\pi i\varepsilon_o\omega}\int_0^\infty \left[e^{-u_o|z-h|} + R_{11}(\lambda)e^{-u_o(z+h)}\right]\frac{\lambda}{u_o}\, J_o(\lambda\rho)d\lambda \qquad (1)$$

where

$$R_{11}(\lambda) = \frac{K_o - Z_1}{K_o + Z_1}, \quad K_o = \frac{u_o}{i\varepsilon_o\omega}, \quad u_o = (\lambda^2 - k_o^2)^{1/2}, k_o = \omega/c ,$$

$$Z_1 = K_1\frac{Z_2 + K_1\tanh v_1h_1}{K_1 + Z_2\tanh v_1h_1}, \quad K_n = \frac{v_n}{g_{hn} + i\varepsilon_{hn}\omega} = \frac{v_n}{\sigma_{hn}} ,$$

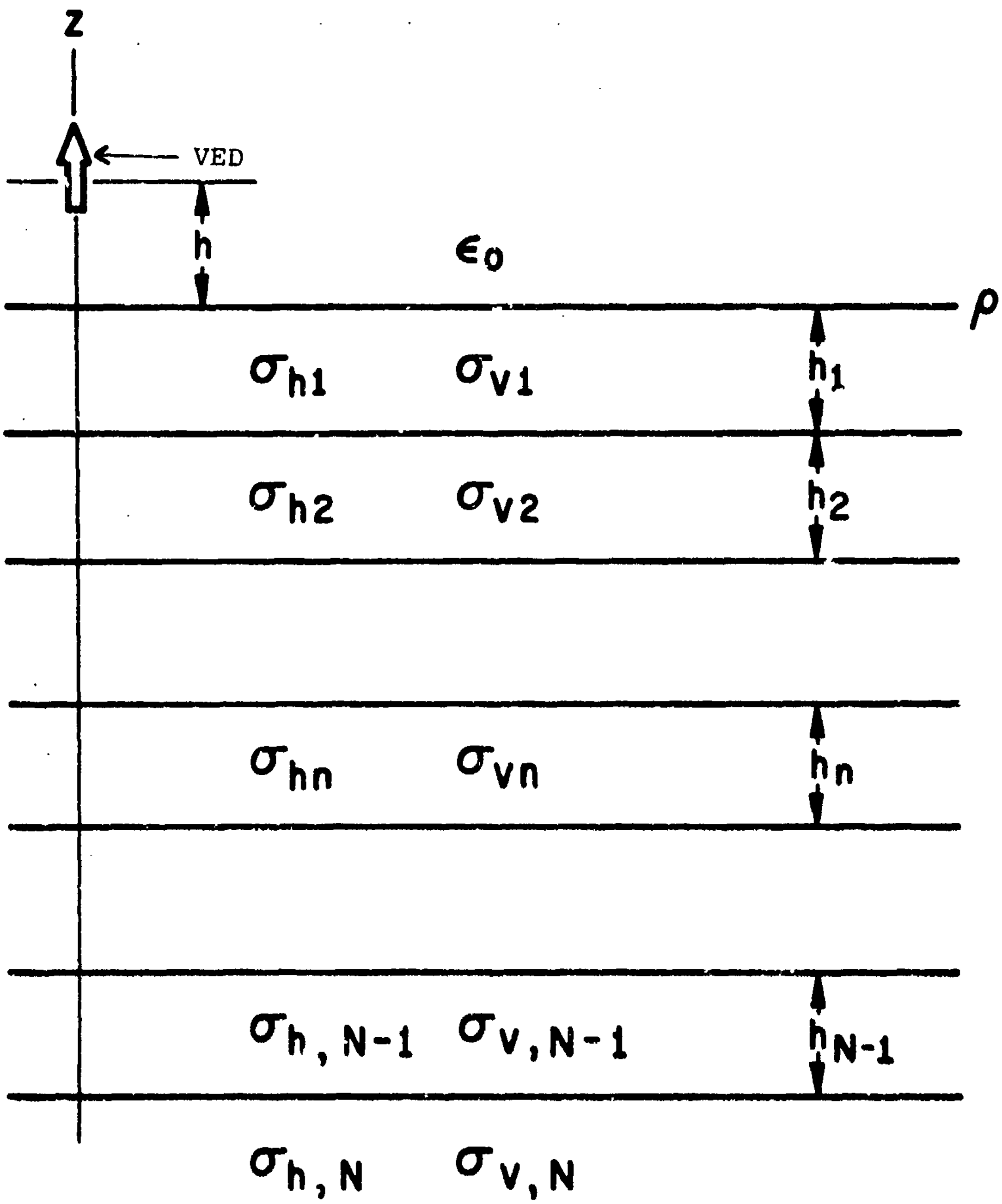

Figure 1

$$Z_2 = K_2 \frac{Z_3 + K_2 \tanh v_2 h_2}{K_2 + Z_3 \tanh v_2 h_2}$$

...

$$Z_n = K_n \frac{Z_{n+1} + K_n \tanh v_n h_n}{K_n + Z_{n+1} \tanh v_n h_n} \quad , \quad n = 1, 2, 3, \ldots N-1$$

$$Z_{N-1} = K_{N-1} \frac{K_N + K_{N-1} \tanh v_{N-1} h_{N-1}}{K_{N+1} + K_N \tanh v_{N-1} h_{N-1}} \quad ,$$

$$v_n = (\lambda^2 \kappa_n + \gamma_n^2)^{1/2}, \quad \kappa_n = \sigma_{hn}/\sigma_{vn} \quad , \quad \gamma_n^2 = i\sigma_{hn}\mu_o\omega \quad .$$

For $z > 0$

$$E_{o\rho} = \frac{\partial^2 \Pi_{oz}}{\partial\rho\partial z} \quad , \quad E_{oz} = k_o^2 + \frac{\partial^2}{\partial z^2} \quad \Pi_{oz} \quad , \quad H_{o\phi} = -i\varepsilon_o\omega \frac{\partial \Pi_{oz}}{\partial\rho} \quad .$$

In the limiting case $z = 0$, we deduce that

$$E_{o\rho} = -\frac{Ids}{4\pi i\varepsilon_o\omega} \int_0^\infty e^{-u_o h} [1 - R_{11}(\lambda)]\lambda^2 J_1(\lambda\rho) d\lambda \quad . \qquad (2)$$

Clearly, this can be used to express the mutual impedance z between a vertical electric dipole of length ds and a horizontal electric dipole of length $d\ell$, as indicated in fig. 2a. Thus,

$$\frac{v}{I} = \frac{E_{o\rho} d\ell \cos\phi}{I} = z \qquad (3)$$

where v is the induced voltage in the element ds and ϕ is the

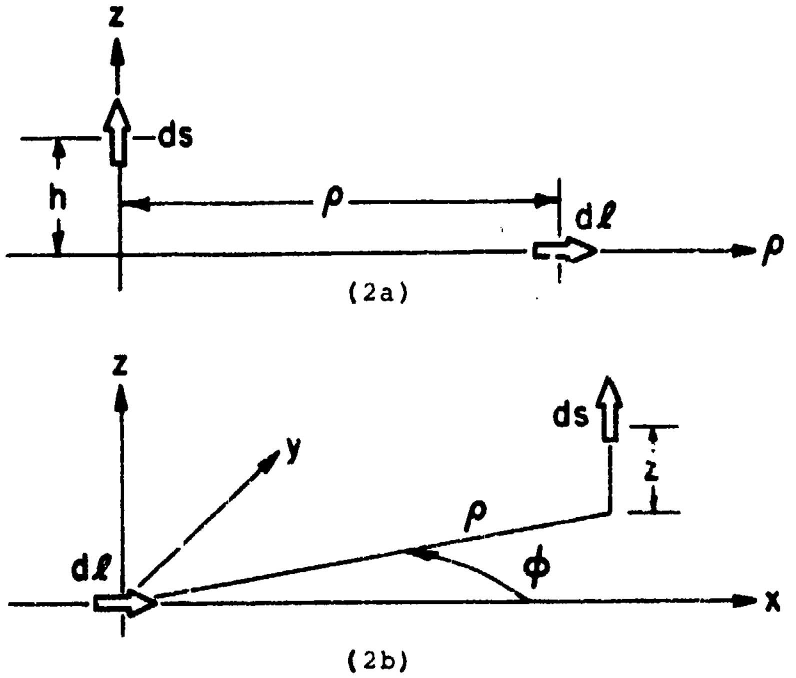

Figure 2

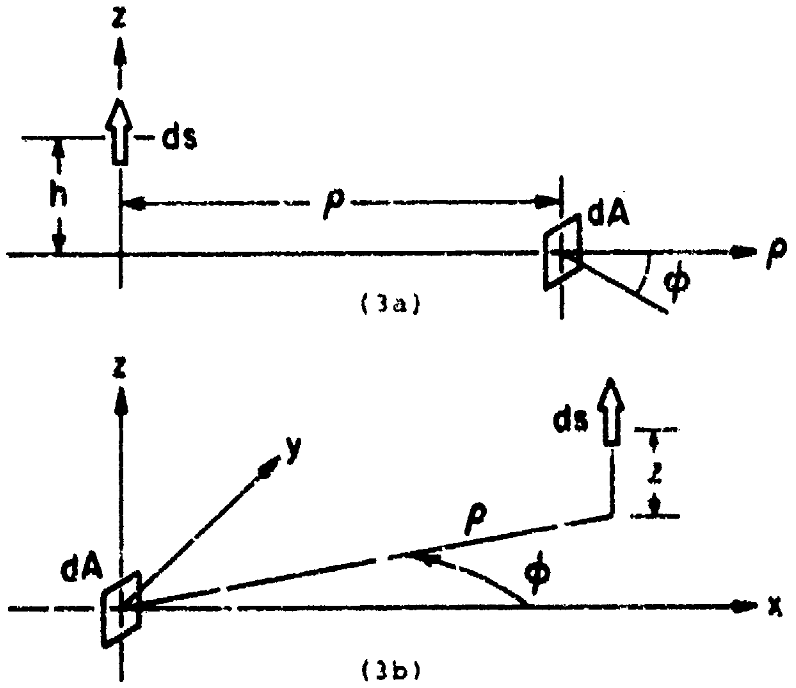

Figure 3

angle subtended by $d\ell$ and the radius ρ. By reciprocity Z the mutual impedance is also defined as

$$Z = \frac{E_{oz} ds}{I} \tag{4}$$

where $E_{oz}ds$ is the voltage in the element ds for a current I in the element $d\ell$. Thus, the vertical electric field E_{oz} at a height z (= h) for a horizontal electric dipole located at the origin of a Cartesian system (x, y, z) and oriented in the positive x direction, as shown in fig. 2b, is

$$E_{oz} = \frac{I d\ell}{4\pi i \varepsilon_o \omega} \int_0^\infty [1 - R_{11}(\lambda)] e^{-u_o z} \lambda^2 J_1(\lambda\rho) d\lambda \cos\phi \quad . \tag{5}$$

Not surprisingly this checks with the field expressions derived directly for the horizontal electric dipole source (Wait, 1967b).

Now consider the magnetic field at z = 0 of the original VED of elemental length $d\ell$. Using (1), it follows that

$$H_{o\phi} = \frac{Ids}{4\pi} \int_0^\infty [1 + R_{11}(\lambda)] e^{-u_o h} \frac{\lambda^2}{u_o} J_1(\lambda\rho) d\lambda \quad . \tag{6}$$

In a similar fashion we can use this to calculate the voltage v induced in a small loop of area dA whose axis subtends an angle ϕ with the radius vector ρ. Thus the mutual impedance is

$$z = \frac{V}{I} = \frac{-iu_o \omega H_{o\phi} dA \sin\phi}{I} \tag{7}$$

where the geometry is shown in fig. 3a, and the minus sign in (7) is a consequence of Faraday's law. But this is the same as

$$z = \frac{E_{oz} ds}{I} \tag{8}$$

where now E_{oz} is the vertical electric feild at the height $z(= h)$ for a horizontal magnetic dipole of moment IdA located at the origin and oriented in the x direction, as shown in fig. 3b. Thus,

$$E_{oz} = \frac{-iu_o \omega IdA}{4\pi} \int_o^\infty [1 + R_{11}(\lambda)] e^{-u_o z} \frac{\lambda^2}{u_o} J_1(\lambda\rho) d\lambda \sin\phi \quad . \tag{9}$$

Now, consider the extension to the case where the VED antenna is located within the top layer (at $z = h$) (i.e., $o>h>-h_1$). Then, for the observer at $z>o$, we have (Wait, 1967b)

$$\Pi_{oz} = \frac{Ids}{4\pi i\epsilon_o \omega} \int_o^\infty g_v^{(1)}(h) [1 + R_{11}(\lambda)] e^{-u_o z} \frac{\lambda}{u_o} J_o(\lambda\rho) d\lambda \quad , \tag{10}$$

where

$$g_v^{(1)}(h) = \frac{i\epsilon_o \omega}{\sigma_{v1}} \left[\frac{e^{v_1 h} + R_{11}^{(1)} e^{-2v_1 h_1} e^{-v_1 h}}{1 + R_{11}^{(1)} e^{-2v_1 h_1}} \right]$$

and

$$R_{11}^{(1)} = \frac{K_1 - Z_2}{K_1 + Z_2} .$$

For $-v_1 h << 1$,

$$g_v^{(1)}(h) \sim \frac{i\omega\varepsilon_o}{\sigma_{v1}} \left(1 - i\sqrt{\gamma_o^2 K_1 - \gamma_1^2}\, \Delta^{(1)} h\right)$$

with

$$\Delta^{(1)} = \frac{1 - R_{11}^{(1)} e^{-2v_1 h_1}}{1 + R_{11}^{(1)} e^{-2v_1 h_1}}$$

$$\gamma_o = ik_o$$

(Wait, 1967b).

An alternative method for deriving the result in equation (1) is to match the boundary conditions using general expressions for the potentials in the various regions. This method yields, for a source within the top layer and observer at $z > 0$,

$$\Pi_{oz} = \frac{Ids}{4\pi\sigma_{v1}} \int_0^\infty \left[\frac{e^{v_1 h} + R_{11}^{(1)} e^{-2v_1 h_1} e^{-v_1 h}}{1 - R_{11}^{(0)} R_{11}^{(1)} e^{-2v_1 h_1}}\right] \frac{2K_o}{K_1 + K_o}\, e^{-u_o z} \frac{\lambda}{u_o} J_o(\lambda\rho)\, d\lambda$$

with

$$R_{11}^{(0)} = \frac{K_1 - K_o}{K_1 + K_o} .$$

Now, after a great deal of algebra, one can show that

$$1 + R_{11}(\lambda) = \frac{2K_o}{K_1 + K_o} \frac{\left(1 + R_{11}^{(1)} e^{-2v_1 h_1}\right)}{1 - R_{11}^{(0)} R_{11}^{(1)} e^{-2v_1 h_1}}$$

and the product $(1 + R_{11}) g_v^{(1)}$ yields the result above. The vertical electric field in the air is readily obtained from (10) by using

$$E_{oz} = (k_o^2 + \partial^2/\partial z^2) \Pi_{oz} \quad .$$

It should be noted that here h is negative, while h_1 is always positive. If the observer is also within the top layer $(o > z > -h_1)$, we have, for $h = 0^-$, that

$$E_z = \frac{Ids}{4\pi i \varepsilon_o \omega} \int_0^\infty g_v^{(1)}(o) g_v^{(1)}(z) [1 + R_{11}(\lambda)] \frac{\lambda^3}{u_o} J_o(\lambda \rho) d\lambda \quad . \quad (11)$$

The required form for $g_v^{(1)}(0)$ follows from the discussion given by Wait (1967a). A further extension is to allow the VED to be located within the second layer (i.e., $-h_1 > h > -h_2$), then for the observer at $z > o$, we deduce that

$$\Pi_{oz} = \frac{Ids}{4\pi i \varepsilon_o \omega} \int_0 g_v^{(2)}(h) [1 + R_{11}(\lambda)] e^{-u_o z} \frac{\lambda}{u_o} J_o(\lambda \rho) d\lambda \quad , \quad (12)$$

where

$$g_v^{(2)}(h) = g_v^{(1)}(-h_1)\frac{v_1}{v_2}\left[\frac{e^{v_2(h+h_1)} + R_{11}^{(2)} e^{-2v_2h_2} e^{-v_2(h+h_1)}}{1 + R_{11}^{(2)} e^{-2v_2h_2}}\right]$$

The corresponding expression for the vertical electric field E_{oz} in the air for $z > 0$ due to the VED source within the second layer is thus

$$E_{oz} = \left(k_o^2 + \frac{\partial^2}{\partial z^2}\right)\Pi_{oz}$$

$$= \frac{Ids}{4\pi i\varepsilon_o\omega}\int_o^\infty g_v^{(2)}(h)\,[1 + R_{11}(\lambda)]\,e^{-u_o z}\,\frac{\lambda^3}{u_o}\,J_o(\lambda\rho)\,d\lambda \quad . \qquad (13)$$

If the observer is now within the second layer (i.e., $-h_i > z > -h_2$), we have

$$E_{2z} = \frac{Ids}{4\pi i\varepsilon_o\omega}\int_o^\infty g_v^{(1)}(o)\,g_v^{(2)}(z)\,[1 + R_{11}(\lambda)\,\frac{\lambda^3}{u_o}\,J_o(\lambda\rho)\,d\lambda \qquad (14)$$

for the case $h = 0^-$. Here we note that $g_v^{(1)}(o) = i\varepsilon_o\omega/\sigma_{v1}$ to account for the location of the VED at and just below the top interface.

Another interesting extension is to consider the source HMD (horizontal magnetic dipole) of moment IdA located in the second layer and the observer also in the air; $z>0$. Here we can deduce that

$$E_{oz} = \frac{i\mu_o \omega I dA}{4\pi} \int_0^\infty g_m^{(2)}(h) e^{-u_o z} [1 + R_{11}(\lambda)] \frac{\lambda^2}{u_o} J_1(\lambda\rho) d\lambda \sin\phi \quad (15)$$

where

$$g_m^{(2)}(h) = g_m^{(1)}(-h_1) \left[\frac{e^{v_2(h+h_1)} + R_{11}^{(2)} e^{-2v_2 h_2} e^{-v_2(h+h_1)}}{1 + R_{11}^{(2)} e^{-2v_2 h_2}} \right] .$$

$$R_{11}^{(2)} = \frac{K_2 - Z_3}{K_2 + Z_3} ,$$

and

$$g_m^{(1)}(z) = \frac{e^{v_1 z} + R_{11}^{(1)} e^{-2v_1 h_1} e^{-v_1 z}}{1 + R_{11}^{(1)} e^{-2v_1 h_1}} .$$

We note here that $g_m^{(1)}$ has the same form as $g_v^{(1)}(z)$ except for the omission of the factor $i\varepsilon_o\omega/\sigma_{v1}$. This follows, since tangential H is continuous while vertical E is discontinuous at an interface.

Now we consider some asymptotics. To illustrate the form of the results, we locate the VED within the second layer and observe the vertical electric field in the air. Then, following Wait (1967b), the dominant far-field approximation to (13) is

$$E_{oz} \simeq \frac{i\mu_o \omega I ds}{2\pi\rho} e^{-ik_o\rho} \bar{g}_v^{(2)}(h)(1 + ik_o z\Delta) W(p) \quad (16)$$

where

$$\bar{g}_v^{(2)}(h) = g_v^{(2)}(h)\Big|_{\lambda = k_o}$$

$$W(p) \simeq -1/(2p)$$

$$p = -ik_o\rho\Delta^2/2$$

$$\Delta = z_1/\eta_o\Big|_{\lambda = k_o} , \quad \eta_o = \sqrt{\mu_o/\varepsilon_o} \cong 120\pi \quad .$$

Higher order terms in the asymptotic expansion of (13) yield

$$E_{oz} \sim \frac{i\omega\mu_o Ids}{2\pi\rho} e^{-ik_o\rho} \bar{g}_v^{(2)}(h) W(p) \times$$

$$\times \left\{1 + ik_o z\Delta + \frac{3}{2p} - \frac{3z}{\Delta\rho} - \frac{3ik_o z^2}{2\rho} + \frac{k_o^2 z^3}{2\rho}\right\} .$$

The term 3/2p agrees with Wait (1964). This is entirely consistent with the formulas for the single slab quoted by Wait (1967b and 1968).

In a similar fashion, from (5), we can deduce the far field E_{oz} for the HED within the second layer. Thus

$$E_{oz} \simeq \frac{i\mu_o\omega Id\ell}{2\pi\rho} e^{-ik_o\rho} \Delta\bar{g}_h^{(2)}(h)(1 + ik_o z\Delta)W(p)\cos\phi \qquad (17)$$

where

$$\bar{g}_h^{(2)}(h) = g_h^{(2)}(h)\Big|_{\lambda = k_o}$$

and

$$g_h^{(2)}(h) = g_h^{(1)}(-h_1)\left[\frac{e^{v_2(h+h_1)} - R_{11}^{(2)} e^{-2v_2h_2} e^{-v_2(h+h_1)}}{1 - R_{11}^{(2)} e^{-2v_2h_2}}\right]$$

and

$$g_h^{(1)}(z) = \frac{e^{v_1z} - R_{11}^{(1)} e^{-2v_1h_1} e^{-v_1z}}{1 - R_{11}^{(1)} e^{-2v_1h_1}} \quad .$$

A similar asymptotic analysis can be carried out for the HMD located within the second layer. From (9) we find that, for $z > 0$,

$$E_{oz} = \frac{-iu_o \omega k_o IdA}{2\pi\rho} e^{-ik_o\rho} \bar{g}_m^{(2)}(h)(1 + ik_o z\Delta) W(p) \sin\phi \qquad (18)$$

where

$$\bar{g}_m^{(2)}(h) = g_m^{(2)}(h)\Big|_{\lambda = k_o} \quad .$$

It can be observed that E_{oz}, given by (16), (17), and (18) has an inverse $(\text{distance})^2$ dependence. This is in accordance with the lateral-wave concept discussed by Wait (1967b), Sachs and Wyatt (1968), and Dence and Tamir (1969) for isotropic slab models.

Extensions of (16), (17), and (18) to the case where the observer is below the air-earth interface are simply achieved by replacing $1 + \Delta i k_0 z$ by the appropriate depth-gain function. For example, the vertical electric field within the second layer $(-h_1 > z > -h_2)$ for an HMD also within the second layer $(-h_1 > h > -h_2)$ is (asymptotically) given by

$$E_{2z} \cong \frac{\mu_0 \omega I dA}{2\pi\rho} e^{-ik_0\rho} \bar{g}_m^{(2)}(h)\bar{g}_v^{(2)}(z) W(p) \sin\phi \quad . \tag{19}$$

This kind of multiplication of depth gain functions is only valid in this asymptotic sense when the direct or "through-the-foliage" propagation path is out of contention. Note that the attenuation function in (19) is again W(p) with p a function of Z_1. This demonstrates the fact that the propagation of the energy is along the air first-layer interface regardless of the location of the source and observer.

A vertical magnetic dipole (loop in the horizontal plane) does not excite a lateral wave; i.e., it excites a ϕ-component of electric field but no z-component.

III. NUMERICAL EXAMPLES

In fig. 4a we show the geometry and parameter values for two terminals located in a single homogeneous isotropic layer. The source is located on the ground at h = -12.2 m and the observer is located in the air at z = 1 m. The magnitude of vertical component of the electric field normalized to twice

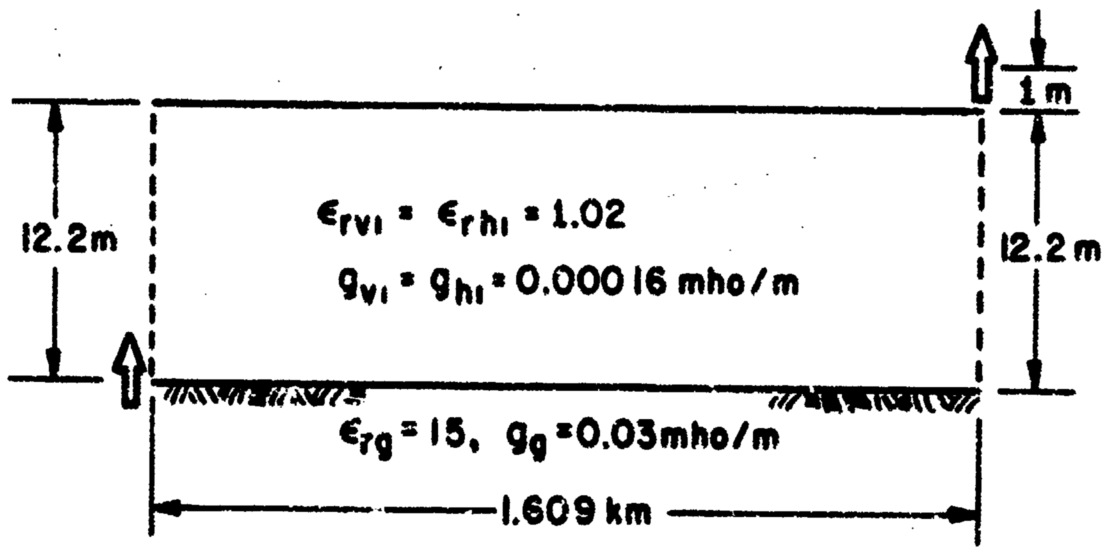
1 m
12.2m
12.2 m
$\epsilon_{rv1} = \epsilon_{rh1} = 1.02$
$g_{v1} = g_{h1} = 0.00016$ mho/m
$\epsilon_{rg} = 15$, $g_g = 0.03$mho/m
1.609 km

Figure 4a

the free-space field

$$E_o = \frac{i\mu_o\omega}{2\pi\rho} e^{-ik_o\rho} \begin{cases} Ids, & \text{VED} \\ Id\ell, & \text{HED} \\ k_o IdA, & \text{HMD} \end{cases}$$

is shown in fig. 4b, plotted versus frequency for the three cases given in equations (16), (17), and (18). We have assumed equal moments, i.e., $Ids = Id\ell = k_o IdA$. This normalization implies the three excitation mechanisms have equal radiation resistance in free space. Also, for the HMD, we have used the maximum value for the azimuthal pattern; i.e., $\varphi = \pi/4$ and the maximum value to the azimuthal pattern of the HED (i.e., $\varphi = 0$). We find from fig. 4b that the VED and HMD have nearly equal signal strengths, while the HED is approximately an order of magnitude smaller. The HED is smaller by the additional factor $\Delta = Z_1/\eta_o$ in equation (17).

In fig. 5a we show the geometry and parameter values for two terminals located in and near two homogeneous, uniaxial-type, anisotropic layers that could account (crudely) for the tree-trunk orientation. The upper layer is isotropic, the lower layer anisotropic. The parameter values for the anisotropic slab were taken from Smith (1969). The anisotropic character of the slab model may simulate the difference between the tree trunks and foliage. The transmitting and receiving antenna heights together with the path length were taken from the Jansky and Bailey data (1965).

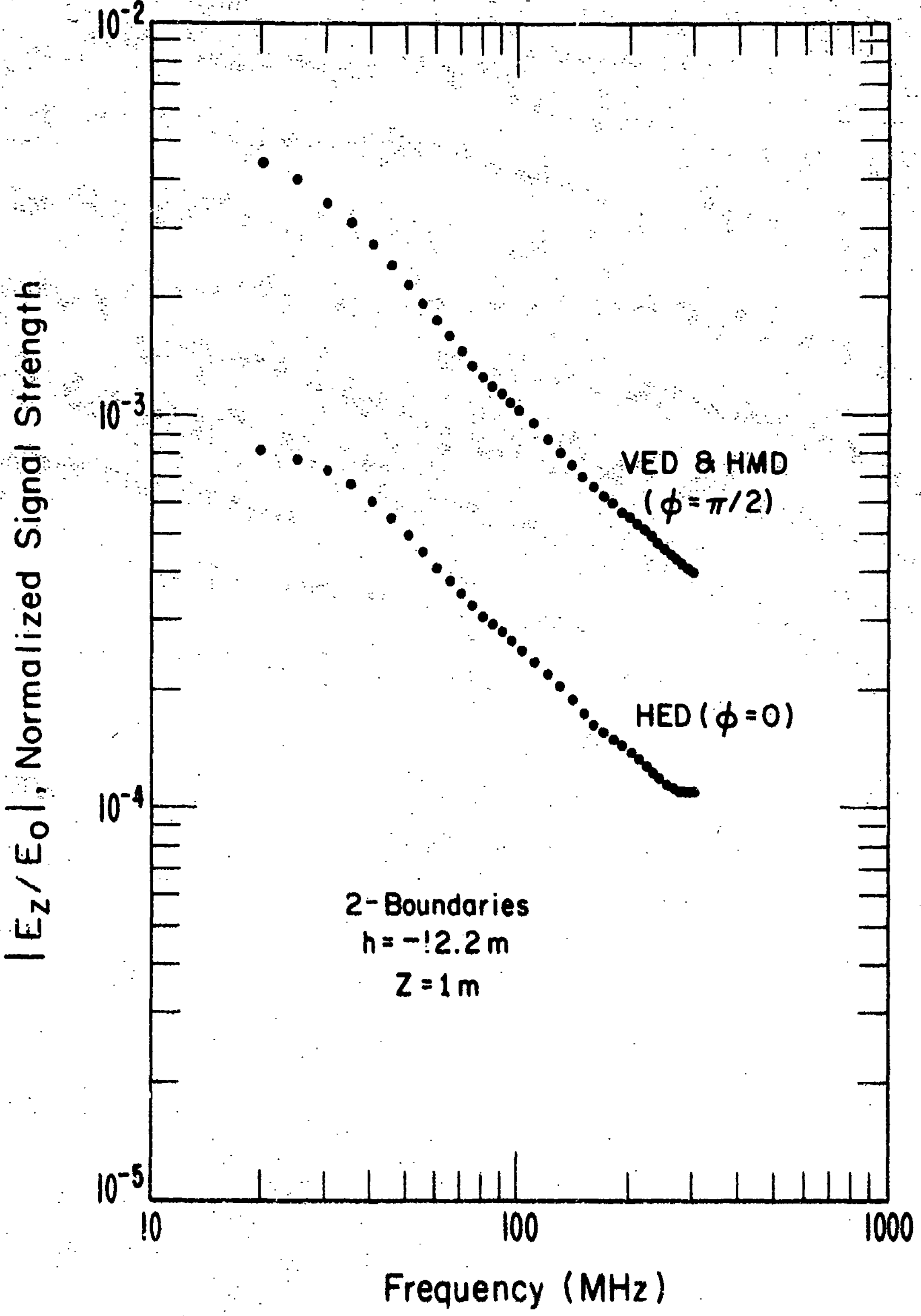

10^-2
10^-3
10^-4
10^-5
|Ez/Eo|, Normalized Signal Strength
VED & HMD
(φ=π/2)
HED (φ=0)
2-Boundaries
h=-!2.2m
Z=1m
!0
100
1000
Frequency (MHz)

Figure 4b

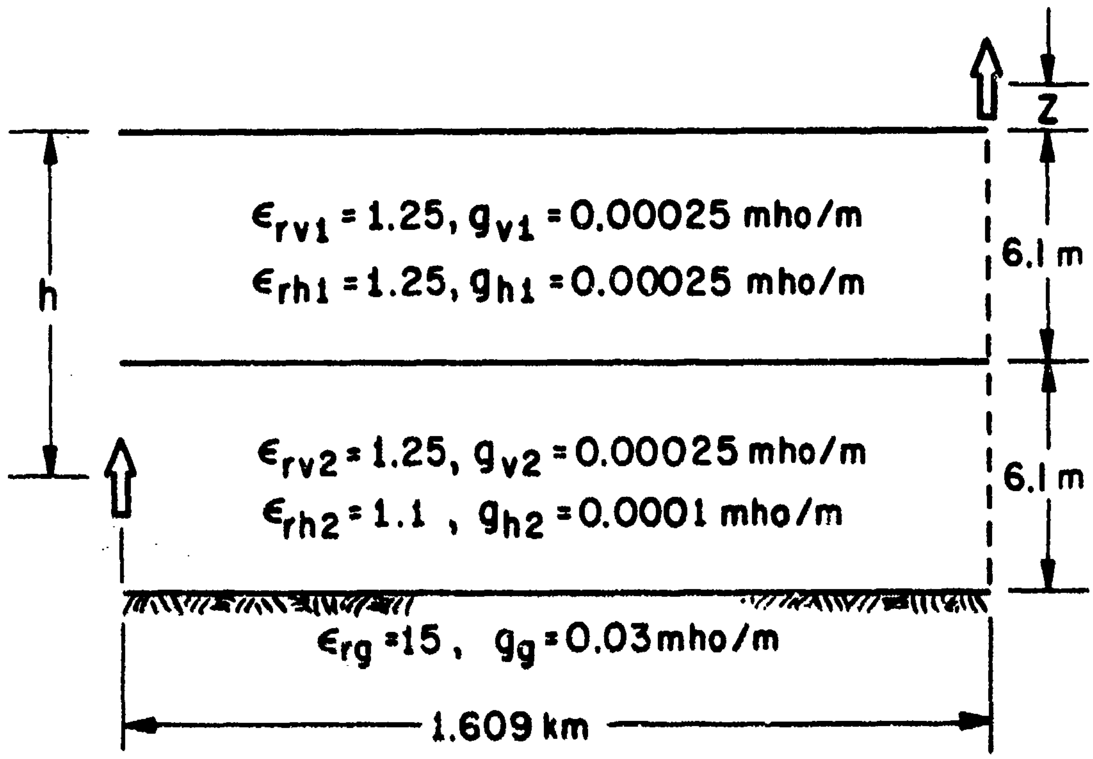
Z
h
ϵ_{rv1} = 1.25, g_{v1} = 0.00025 mho/m
ϵ_{rh1} = 1.25, g_{h1} = 0.00025 mho/m
6.1 m
ϵ_{rv2} = 1.25, g_{v2} = 0.00025 mho/m
ϵ_{rh2} = 1.1 , g_{h2} = 0.0001 mho/m
6.1 m
ϵ_{rg} = 15 , g_g = 0.03 mho/m
1.609 km

Figure 5a

In fig. 5b the magnitude of the vertical component of electric field is plotted for the three excitation mechanisms versus frequency. Again, the maximum in the azimuthal patterns for the HED and HMD were used. The observer is located just above the top layer. The HMD and VED have nearly equal signal strengths, while the HED is about an order of magnitude smaller.

In fig. 5c we show the effect of elevating the transmitting antenna (VED in this case) to h = -8.2 m. We see from fig. 5c that the signal strength for the elevated transmitter is somewhat greater toward the higher end of the frequency range. However, at many frequencies, the signal strength for the transmitter at h = -12.2 is comparable with the signal strength at h = -8.2 m. In fig. 5d we show the effect of having both terminals in the second layer where the vertical component of the electric field is plotted versus frequency for two cases: 1) the source in the 2nd layer of fig. 5a, at h = -12.2m and the observer in the air at z = 1 m, and 2) the source and observer in the 2nd layer at h = -12.2 m, z = -12.2 m. In this case, equation (16) is modified to account for the location of the observer in the 2nd layer as

$$E_{2z} \approx \frac{i\omega\mu_o Ids}{2\pi\rho} e^{-ik_o\rho} \bar{g}_v^{(2)}(h)\bar{g}_v^{(2)}(z)W(p).$$

The reduction in signal strength when both transmitter and receiver are in the second layer is evident in fig. 5d. In

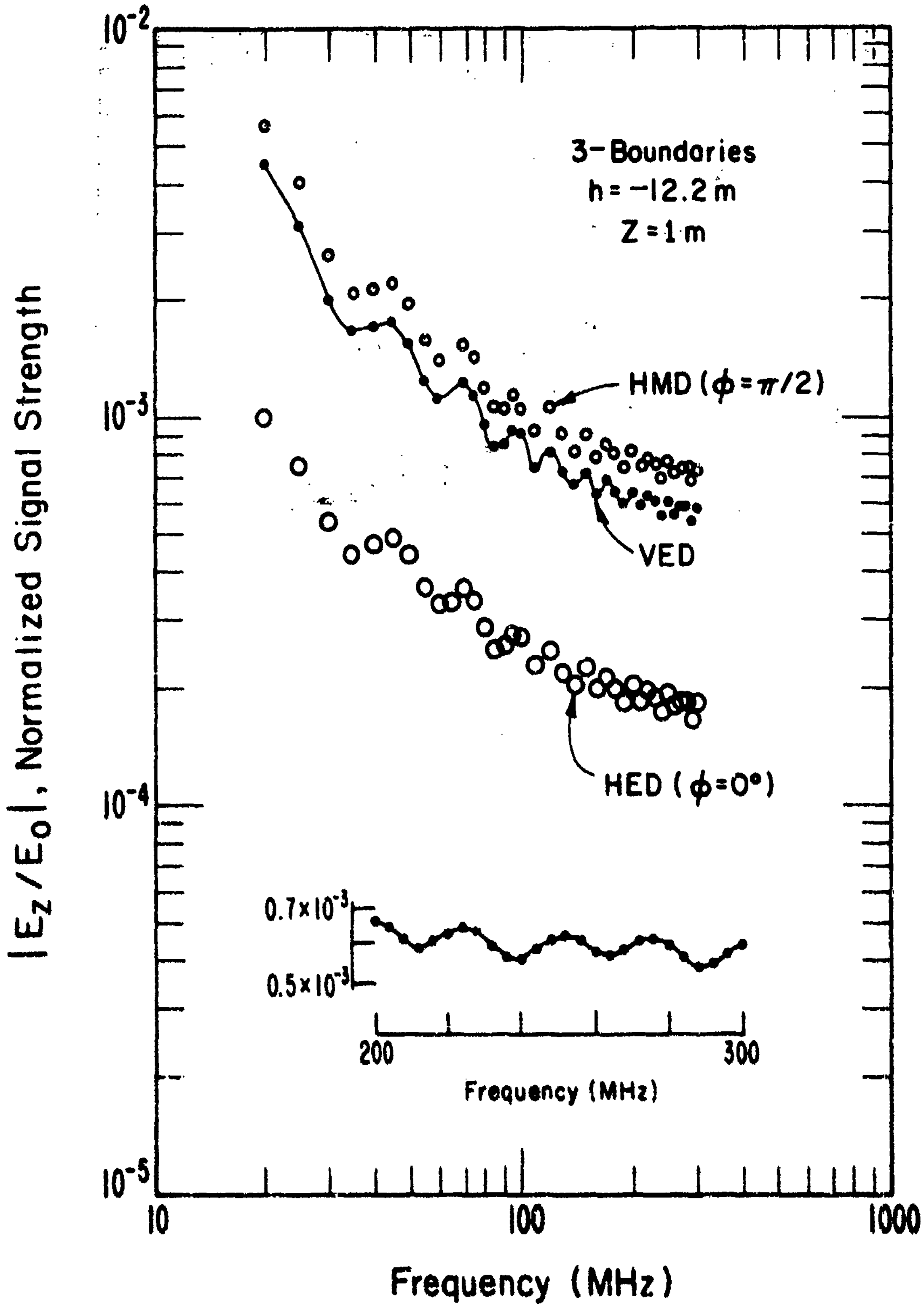
3-Boundaries
h = -12.2 m
Z = 1 m
HMD (φ = π/2)
VED
HED (φ = 0°)
0.7×10⁻³
0.5×10⁻³
200
300
Frequency (MHz)
10^{-2}
10^{-3}
10^{-4}
10^{-5}
10
100
1000
Frequency (MHz)
$|E_z/E_o|$, Normalized Signal Strength

Figure 5b

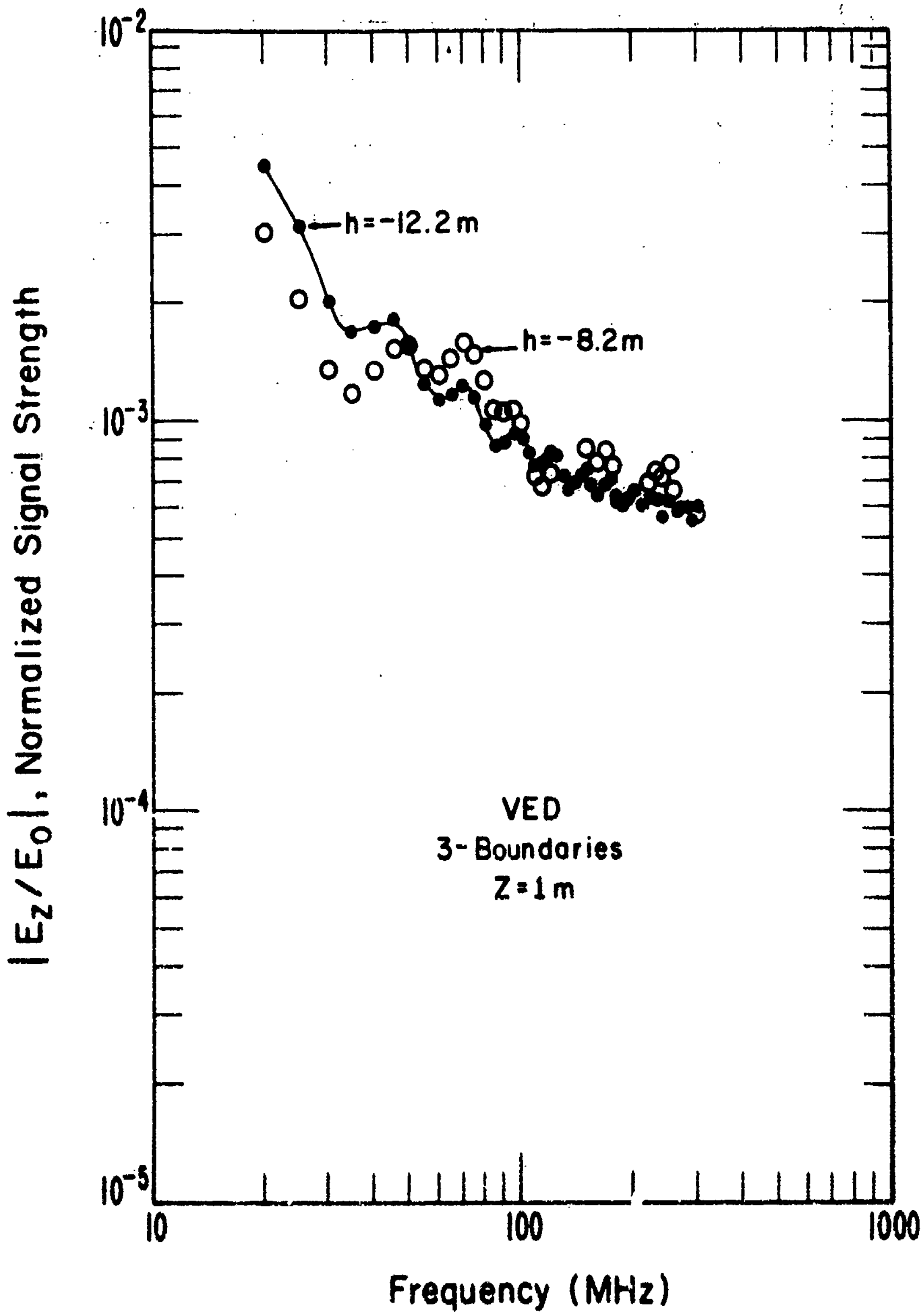

10^{-2}
10^{-3}
10^{-4}
10^{-5}
10
100
1000
h=-12.2m
h=-8.2m
VED
3-Boundaries
Z=1m
|Ez/Eo|, Normalized Signal Strength
Frequency (MHz)

Figure 5c

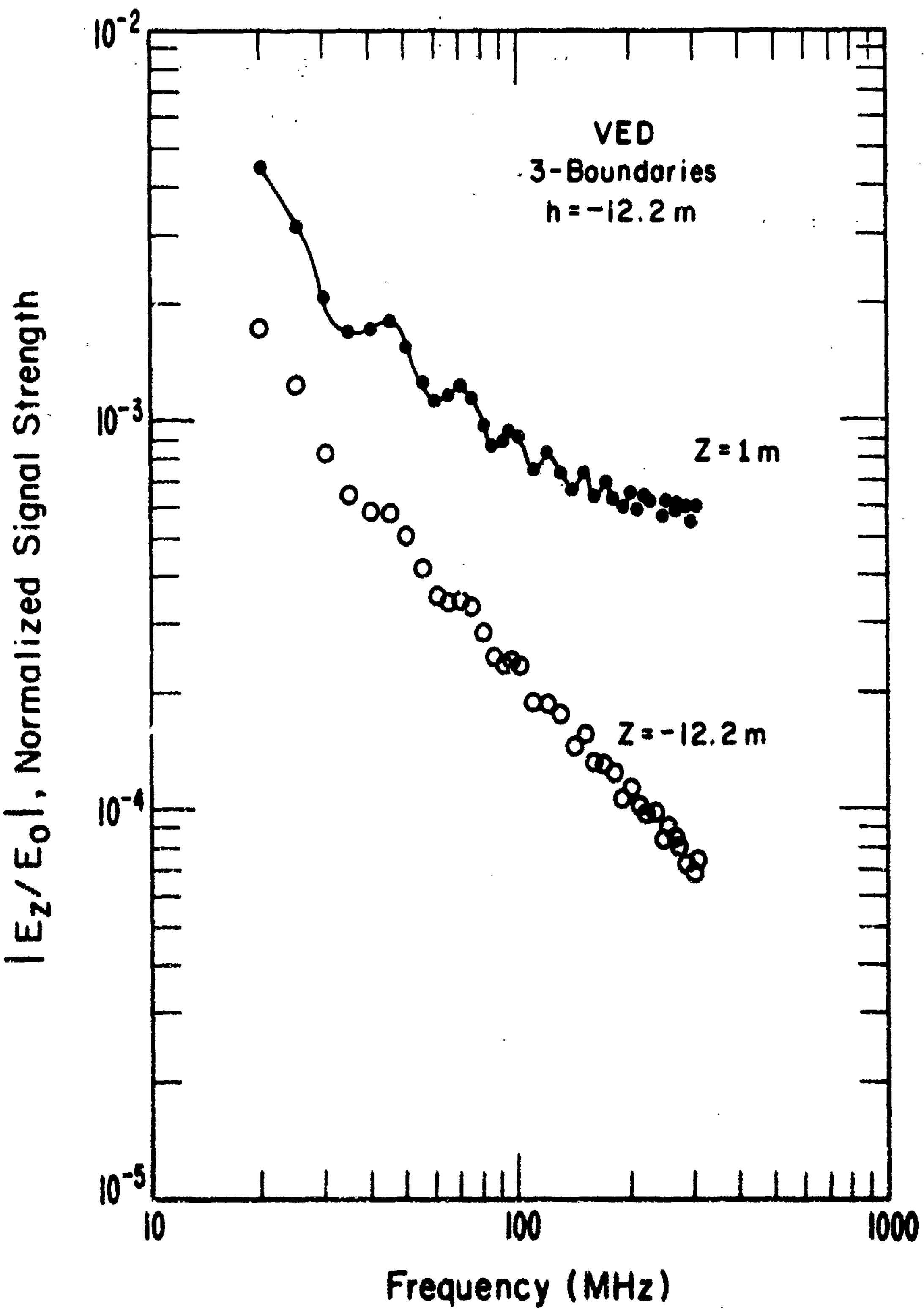
VED
3-Boundaries
h = -12.2 m
Z = 1 m
Z = -12.2 m
10^{-2}
10^{-3}
10^{-4}
10^{-5}
10
100
1000
Frequency (MHz)
$|E_z/E_o|$, Normalized Signal Strength

Figure 5d

fig. 6 we show a comparison of theory, as described in this report, with a set of Jansky and Bailey measured data selected at random. The predicted and measured basic transmission loss, defined as

$$\text{Basic Transmission Loss} = -20\log_{10}|2E_z/E_o| + 20\log_{10}(2k_o\rho) \tag{20}$$

is plotted versus frequency in fig. 6. At 20 MHz, the predicted and measured values differ by about 3 dB. As the frequency increases above 20 MHz, the difference between theory and measured basic transmission loss increases to about 18 dB at 50 MHz. From 50 MHz to 300 MHz, the difference between theory and measured basic transmission loss remains constant and equal to about 18 dB. It is interesting that the theory predicts the greater loss. A possible explanation for the discrepancy between theory and measured data in fig. 6 may be the measured data were taken with the receiving antenna located on a tower in a partial clearing. At low frequencies, a partial clearing would be indistinguishable to the wave from the jungle itself. As the frequency is increased, the transition from jungle to clearing is more abrupt. As the frequency is increased still further, the loss will increase at a constant rate corresponding to one term in the residue series representation for the field strength, E_z. That is, for sufficiently high frequencies, and $z = h = 0$,

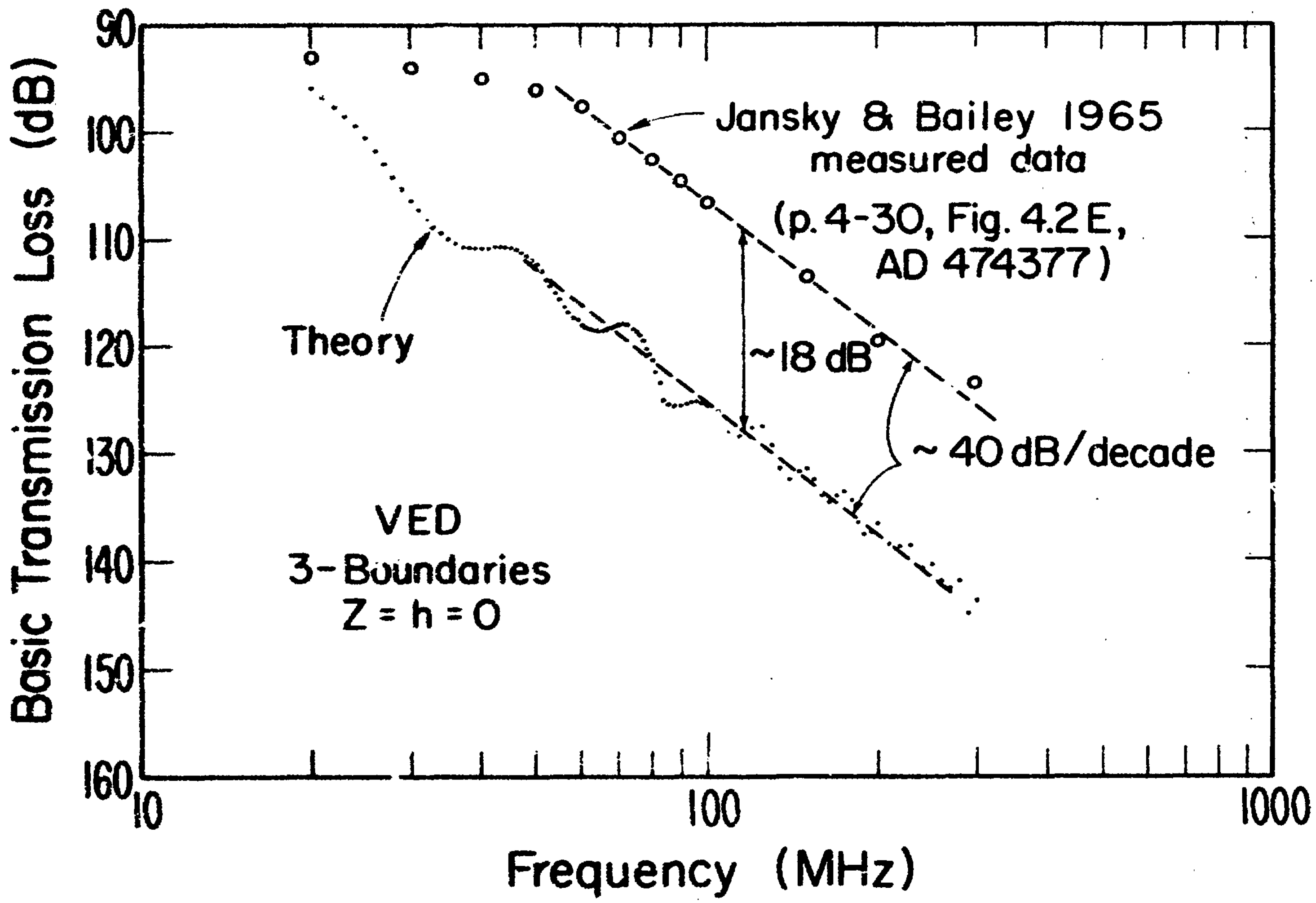
Basic Transmission Loss (dB)
90
100
110
120
130
140
150
160
10
100
1000
Frequency (MHz)
Jansky & Bailey 1965
measured data
(p. 4-30, Fig. 4.2 E,
AD 474377)
Theory
~18 dB
~ 40 dB/decade
VED
3-Boundaries
Z = h = 0

Figure 6

$$\left|\frac{E_z}{E_o}\right| \underset{f\to\infty}{\sim} \frac{1}{k_o \rho |\Delta|^2} \quad . \tag{21}$$

In fig. 6, ρ is constant and equal to 1.609 km, and at sufficiently high frequencies, Δ becomes

$$\Delta \underset{f\to\infty}{\sim} \frac{\sqrt{\varepsilon_r - 1}}{\varepsilon_r} \quad .$$

Substituting (21) into (20) gives

$$\text{Basic Transmission Loss} \underset{f\to\infty}{\sim} 40 \log_{10} f \tag{22}$$

which is shown as 40 dB/decade in fig. 6. The frequency dependence is more complicated when either the source or observer is located within the slab. It is encouraging that both theory and measured data obey the 40-dB loss per decade principle. The fact that both fall off as 40 dB/decade seems to indicate the validity of the slab model for jungle propagation.

Another possible explanation for the discrepancy in fig. 6 between theory and measured data is the choice of constitutive parameters in fig. 5a. It may be possible by selecting a different combination of these parameters to bring the theory in closer agreement with the measured data in fig. 6.

Both the effects of a partial clearing and selection of constitutive parameters for modeling a jungle need further study before the slab model can be used for making path loss predictions.

Wait (1968) gives the optimum inclination angle for the tilted electric dipole in terms of the index of refraction, thickness of the upper layer, and the burial depth. This optimum angle minimizes the transmission loss of the lateral-wave component. Since the VMD does not excite a vertical component of E, the loop has no optimum inclination angle as does the dipole.

IV. CONCLUSIONS

Simple closed form expressions for the lateral wave excited by loops and dipoles in or above a foliage layer are derived. The model of the foliage layer may consist of an arbitrary number of homogeneous, uniaxial, anisotropic layers.

For the example considered, the vertical electric dipole and the horizontal magnetic dipole (loop in vertical plane) have nearly equal signal strengths, while the horizontal electric dipole strength is approximately an order of magnitude smaller. Also, it is desirable to elevate both antennas to as near the top of the foliage layer as possible to minimize the transmission loss.

V. ACKNOWLEDGMENT

The programming assistance of Mr. Duane C. Hyovalti was a valuable addition to this study. Also, Mr. George C. Lane provided valuable information.

REFERENCES

Dence, D., and T. Tamir (1969), Radio loss of lateral waves in forest environments, Radio Sci. 4, No. 4, 307-318.

Herbstreit, J. W., and W. Q. Crichlow (1964), Measurement of the attenuation of radio signals by jungles, Radio Sci. J. Res. 68D, No. 8, 903-906.

Ikrath, K., and G. LeMarne (1971), Modeling of HF-VHF radio transmission in jungle forest covered terrains, U. S. Army Electronics Command, Fort Monmouth, NJ 07703, Tech. Rept. ECOM-3512, Nov.

Jansky and Bailey Engr. Dept. of Atlantic Res. Corp. (1965), Tropical Propagation Research, Semiannual Rept. #6, Contract No. DA36-039, SC-90889, AD474-377.

Jones, J., and L. G. Sturgill (1965), Tropical propagation research, Semiannual Repts. 4, 5, and 6, Jansky and Bailey, Atlantic Res. Corp., Alexandria, VA (unpublished).

Lippman, B. A. (1965), The jungle as a communication network, Internal Memo., Defense Res. Corp., P.O.Box 3587, Santa Barbara, CA 93105.

Sachs, D. L. (1966), A conducting-slab model for electromagnetic propagation within a jungle medium, II. Internal Memo. #471, Defense Res. Corp., P. O. Box 3537, Santa Barbara, CA 93105, AD711953, Sept.

Sachs, D. L. (1969), Theory of radio propagation in a jungle environment, Tech. Memo. 1011, General Res. Corp., P. O. Box 3587, Santa Barbara, CA 93105, AD857100, Jan.

Sachs, D. L., and P. J. Wyatt (1968), A conducting-slab model for electromagnetic propagation within a jungle medium, Radio Sci. 3, No. 2, 125-134

Smith, G. W. (1969), A general computer model of radio communication link performance, General Res. Corp., P.O. Box 3587, Santa Barbara, CA 93105, Jan., 20-28.

Staiman, D., and T. Tamir (1966), Nature and optimisation of the ground (lateral) wave excited by submerged antennas, Proc IEE 113, No. 8, 1299-1310.

Tamir, T. (1967), On radio-wave propagation in forest environments, IEEE Trans. Ant. Prop. AP-15, No. 6, Nov., 806-817.

Tamir, T., and L. B. Felsen (1964), On the relation between pole waves and lateral waves in slab configurations, PIB Res. Rept. No. PIBMRI-1245-64, AD610584, Brooklyn, NY, Nov.

Wait, J. R. (1964), Electromagnetic Surface Waves, reprinted from Advances in Radio Research (ed., J. A. Saxton), Vol. 1, 157-217 (Academic Press, New York), p. 162, ex. (12).

Wait, J. R. (1966), Fields of a horizontal dipole over a stratified anisotropic half-space, IEEE Trans. Ant. Prop. AP-14, No. 6, 790-792.

Wait, J. R. (1967a), Radiation from dipoles in an idealized jungle environment, Radio Sci. 2, No. 7, 747-750. (Note, in eq. (1) replace $R_{||}(\lambda)\exp(u_0(Z+h))$ with $R_{||}(\lambda)\exp(-u_0(Z+h))$.

Wait, J. R. (1967b), Asymptotic theory for dipole radiation in the presence of a lossy slab lying on a conducting half space, IEEE Trans. Ant. Prop. AP-15, No. 5, 645-648. (Note that $r_{||}$ and $r_{\perp}$, as defined on p.647, have a missing minus sign. Also, in eq. (6), the plus sign between the two fractions within the braces (i.e., the fractions with exponential functions in the numerator) should be replaced with a minus sign. Also, the factor λ/u_o in (13) only is spurious.)

Wait, J. R. (1968), Optimization of the ground wave over a stratified earth, Electron. Letters 4, No. 26, 575-576.